Journal of Medicinal Chemistry Article

J. Med. Chem. **2010,** *53,* 5549–5557 **5549**
DOI: 10.1021/jm100269c

Synthesis, Fluorine-18 Radiolabeling, and Biological Evaluation of *N*-((*E*)-4-Fluorobut-2-en-1-yl)-2β-carbomethoxy-3β-(4′-halophenyl)nortropanes: Candidate Radioligands for In Vivo Imaging of the Brain Dopamine Transporter with Positron Emission Tomography

Jeffrey S. Stehouwer,[†] Lauryn M. Daniel,[†] Ping Chen,[†] Ronald J. Voll,[†] Larry Williams,[†] Susan J. Plott,[‡] John R. Votaw,[†] Michael J. Owens,[‡] Leonard Howell,[‡,§] and Mark M. Goodman*[,†,‡]

[†]*Department of Radiology,* [‡]*Department of Psychiatry and Behavioral Sciences, and* [§]*Yerkes National Primate Research Center, Emory University, Atlanta, Georgia*

Received March 1, 2010

The *N*-(*E*)-fluorobutenyl-3β-(*para*-halo-phenyl)nortropanes **9**−**12** were synthesized as ligands of the dopamine transporter (DAT) for use as ^{18}F-labeled positron emission tomography (PET) imaging agents. In vitro competition binding assays demonstrated that compounds **9**−**12** have a high affinity for the DAT and are selective for the DAT compared to the serotonin and norepinephrine transporters. MicroPET imaging with [^{18}F]**9**−[^{18}F]**11** in anesthetized cynomolgus monkeys showed high uptake in the putamen with lesser uptake in the caudate, but significant washout of the radiotracer was only observed for [^{18}F]**9**. PET imaging with [^{18}F]**9** in an awake rhesus monkey showed high and nearly equal uptake in both the putamen and caudate with peak uptake achieved after 20 min followed by a leveling-off for about 10 min and then a steady washout and attainment of a quasi-equilibrium. During the time period 40−80 min postinjection of [^{18}F]**9**, the ratio of uptake in the putamen and caudate vs cerebellum uptake was ≥4.

Introduction

The human dopamine transporter (DAT[a]) is a 620-amino acid transmembrane protein which belongs to the family of Na^+/Cl^- dependent transporters.[3,4] In the central nervous system (CNS), the DAT is located on presynaptic neurons and functions to remove the neurotransmitter dopamine from the synapse, thereby terminating the signaling action of dopamine.[5,6] The DAT is found in high densities in certain brain regions which include the putamen, caudate, nucleus accumbens, and olfactory tubercle, whereas lower densities are found in the substantia nigra, amygdala, and hypothalamus.[7,8] Several neuropsychiatric disorders have been associated with the DAT including Parkinson's disease (PD),[9−11] attention-deficit hyperactivity disorder (ADHD),[12] supranuclear palsy,[10] and Tourette's syndrome.[13] The ability to image the DAT with positron emission tomography (PET) may aid in the diagnosis, monitoring, and treatment of these diseases by providing a means to study the DAT in vivo and by allowing for the in vivo measurement of DAT density in specific brain regions.[14] Furthermore, a suitable DAT PET tracer can be used to measure the occupancy of DAT therapeutics[15] and may facilitate the development of new DAT therapeutics.[16]

The DAT is also the target of several drugs of abuse including cocaine,[17,18] amphetamines, and MDMA (ecstasy), and this has led to the search for compounds that can be employed as potential cocaine addiction therapeutics.[19,20] From this research evolved the 3β-phenyl tropane class of DAT ligands of which compounds **1**−**6** were the first to be prepared.[21−24] These compounds have since been exploited for PET imaging due to the ability to radiolabel with carbon-11 on either the *N*-methyl group or the *O*-methyl ester.[25−28] Carbon-11 has a half-life of 20.4 min, which limits the use of ^{11}C-labeled tracers to the location where they are prepared and to imaging sessions of about 2 h. Fluorine-18 has a half-life of 109.8 min, which allows for longer radiosynthesis times and imaging sessions, and also for the transport of the ^{18}F radiotracer to PET imaging facilities that do not have onsite cyclotrons. Additionally, ^{18}F positrons have a lower maximum energy (0.64 MeV)[29] than ^{11}C positrons (0.97 MeV), which therefore deposits less energy into tissue and also results in a positron with a shorter linear range which allows for higher spatial resolution.[30,31] These physical properties of ^{18}F are serendipitous due to the increasingly valuable role that ^{19}F is playing in medicinal chemistry,[32−35] and a variety of synthetic methods have now been developed to incorporate ^{18}F or ^{19}F into molecules.[36−38]

Out of compounds **1**−**6**, only compound **2** has the potential to be radiolabeled with ^{18}F. Thus, [^{18}F]**2** was prepared and evaluated in rats[39] and humans.[40] In humans, the peak uptake of [^{18}F]**2** in the putamen and caudate occurred at 225 min, followed by a slow washout. Although [^{18}F]**2** showed high uptake in the striatum and the aryl−fluorine bond was found to be metabolically stable to defluorination, the time to peak uptake was considered to take too long and so [^{18}F]**2** was not an optimal DAT PET tracer. Numerous other fluorinated derivatives of **1**−**6**, which contain the ^{18}F-radiolabel as an *N*-fluoroalkyl group or an *O*-fluoroalkyl ester have also been prepared and evaluated.[41] Among the numerous derivatives

*To whom correspondence should be addressed. Phone: (404) 727-9366. Fax: (404) 712-5689. E-mail: mgoodma@emory.edu. Address: Department of Radiology, Wesley Woods Health Centers 2nd floor, 1841 Clifton Road NE, Atlanta, Georgia 30329.

[a]Abbreviations: PET, positron emission tomography; SUV, standardized uptake value;[1,2] TAC, time−activity curve; HRRT, high resolution research tomograph; SERT, serotonin transporter; DAT, dopamine transporter; NET, norepinephrine transporter.

Published on Web 07/02/2010

reported, compounds **7** (FECNT)[42] and **8** (FPCIT)[43] emerged as viable DAT PET tracers and have found use in human PET imaging.[44−50] Both compounds [^{18}F]**7** and [^{18}F]**8** achieve a high uptake and specific binding in the putamen and caudate but neither compound washes out significantly during the course of the study, which is needed to enable kinetic modeling of the tracer behavior.[51,52] Compound **8** also has a higher binding affinity at the serotonin transporter (SERT) than the DAT,[53] and so [^{18}F]**8** is not a DAT-specific PET tracer. Additionally, [^{18}F]**8** defluorinates, which is similar to other tracers containing an [^{18}F]fluoropropyl group,[54−56] whereas [^{18}F]**7** is metabolized to a polar radiometabolite,[57] which can cross the blood−brain barrier (a similar result was recently reported for the amyloid imaging agent [^{18}F]FDDNP[58]). Thus, further improvements are still needed in order to obtain a DAT-selective ^{18}F-labeled PET tracer that can achieve peak uptake, binding equilibrium, and washout in a relatively short period of time while also not defluorinating or producing radiolabeled metabolites that can cross the blood−brain barrier.

We have previously reported the *N*-(*E*)-fluorobutenyl compounds **9**−**12** along with preliminary in vitro binding data and rat biodistribution data.[59,60] The rationale for the *N*-(*E*)-fluorobutenyl group was based upon the characterization and imaging properties of the iodine-123 DAT imaging agent *N*-((*E*)-3-[^{123,125}I]iodopropen-1-yl-2β-carbomethoxy-3β-(4-chlorophenyl)nortropane (MMG-142E/IPT),[61] which showed nanomolar DAT affinity and high striatal to cerebellar ratios with relatively fast washout kinetics, indicating reversible binding, in nonhuman and human primates.[62,63] We hypothesized that the *N*-(*E*)-4-[^{18}F]fluorobut-2-en-1-yl group would serve as a bioisostere for the *N*-(*E*)-3-[^{123,125}I]iodopropen-1-yl group for a new class of DAT PET imaging agents. The preliminary binding data of compounds **9**−**12** demonstrated that the (*E*)-configuration of the fluorobutenyl group was the more biologically active configuration and also that halo-substitution of the phenyl ring resulted in higher binding affinity at the DAT when compared to the unsubstituted phenyl group. Subsequently, the *para*-methyl analogue **13** was reported[64] and, recently, several related derivatives have been reported.[65,66] Herein we report the synthesis and binding affinity determination of **9**−**12** (along with **13** for comparison) in conjunction with the microPET imaging of [^{18}F]**9**−[^{18}F]**11** and [^{18}F]**13** in anesthetized cynomolgus monkeys and the high resolution research tomograph (HRRT) imaging of [^{18}F]**9** in an awake rhesus monkey.[67]

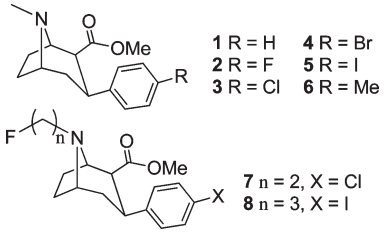

Chemistry

The *N*-(*E*)-fluorobutenyl nortropanes **9**−**13** were synthesized by reacting the appropriate nortropane[24,25,68] with (*E*)-4-fluoro-1-tosyloxy-2-butene (**14**) (Scheme 1). Compound **14** was prepared from *trans*-1,4-dibromo-2-butene (**15**) as shown in Scheme 1. Reaction of **15** with KOAc in AcOH according to the literature procedure[69,70] afforded the diacetoxy compound

Scheme 1

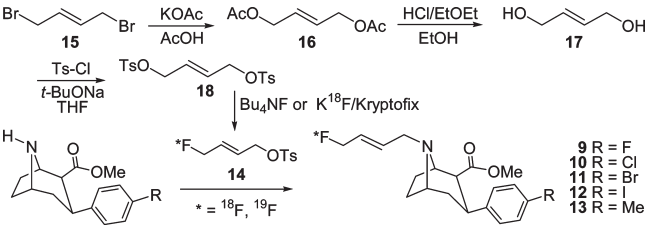

Table 1. Octanol/Water Partition Coefficients

compd	log $P_{7.4}$[a]	*n*
[^{18}F]**9**	1.95 ± 0.01	8
[^{18}F]**10**	2.21 ± 0.02	7
[^{18}F]**11**	2.33 ± 0.03	8

[a] Average value of *n* determinations ± the standard deviation.

16, which was purified on silica rather than by the traditional distillation method. Acid-catalyzed ethanolysis of **16** afforded the diol **17** in nearly quantitative yield. Thus, this method provides a simplified synthesis of diol **17**, which avoids the previously reported LAH reduction of 2-butyne-1,4-diol[71] or DIBAL reduction of a dialkyl fumarate.[72,73] Diol **17** was reacted with tosyl chloride to give ditosylate **18**, which was then reacted with tetrabutylammonium fluoride to give **14**.

Radiochemistry

Compound [^{18}F]**14** was obtained by reacting **18** with K^{18}F/Kryptofix-222 complex in CH_3CN. Following preparation of [^{18}F]**14**, a DMF-solution of the appropriate nortropane[24,25,68,74] was added, the mixture was heated at 105 °C for 15 min, and then purified by semipreparative HPLC. The desired HPLC fractions were combined and diluted with H_2O, and the product was then isolated from this solvent mixture by solid-phase extraction according to a previously reported procedure.[75] The radiotracer was then formulated as a 10% EtOH/saline solution. The octanol/water partition coefficients[76,77] of [^{18}F]**9**−[^{18}F]**11** were measured according to a previously reported procedure,[78,79] and the results are shown in Table 1. These values are all in the range of log P = 1−3, which allows for passive diffusion of the radiotracer across the blood−brain barrier. As expected, the lipophilicity of each radiotracer increases with increasing lipophilicity of the halogen substituent.

In Vitro Competition Binding Assays

The binding affinities of **2** and the *N*-(*E*)-fluorobutenyl nortropanes **9**−**13** to human monoamine transporters (Table 2) were determined using in vitro competition binding assays with membranes prepared from cells transfected with the human SERT, DAT, or norepinephrine transporter (NET) according to our previously reported procedure.[80,81] Compounds **2** and **9**−**13** were screened as the free bases whereas salts were used for the control compounds: cocaine·HCl (DAT), (*S*)-citalopram·oxalate[82] (SERT), and desipramine·HCl[83] (NET). The competing ligands employed were [^{3}H](*R*,*S*)-citalopram·HBr[84] (SERT), [^{125}I]RTI-55[23] ([^{125}I]**5**, DAT), or [^{3}H]nisoxetine[85] (NET).

Compound **12**, which is the *N*-(*E*)-fluorobutenyl analogue of **5** (RTI-55/β-CIT), has a high affinity for the DAT as well as for the SERT and thus displays only a 4-fold selectivity for the DAT over the SERT (this lack of selectivity is very similar to that of **5**[53,86]). Compounds **10** and **11** also have a high DAT

Table 2. Results of In Vitro Competition Binding Assays with Transfected Human Monoamine Transporters[a]

	K_i (nM)[b]			DAT selectivity	
compd	hDAT	hSERT	hNET	SERT/DAT	NET/DAT
9	9.5 ± 2.6^{e}	357.4 ± 193.0^{h}	2607 ± 1432^{e}	~ 38	~ 274
10	0.6 ± 0.3^{d}	11.3 ± 6.4^{i}	142 ± 30^{f}	~ 19	~ 237
11	0.4 ± 0.0^{d}	8.5 ± 0.8^{e}	87 ± 8^{c}	~ 21	~ 218
12	0.5 ± 0.2^{d}	2.2 ± 1.1^{e}	145 ± 125^{e}	~ 4	~ 290
13	2.7 ± 0.1^{d}	147.0 ± 79.3^{j}	265 ± 146^{f}	~ 54	~ 98
2	10.6 ± 0.8^{c}	N/D	N/D	N/A	N/A
cocaine·HCl	46.3 ± 13.5^{d}	N/D	N/D	N/A	N/A
(*S*)-citalopram·oxalate	N/D	1.0 ± 0.6^{g}	N/D	N/A	N/A
desipramine·HCl	N/D	N/D	0.8 ± 0.7^{c}	N/A	N/A

[a] N/A = not applicable. N/D = not determined. [b] Geometric mean of n determinations ± the standard deviation (each determination performed in triplicate). [c] $n = 2$. [d] $n = 3$. [e] $n = 4$. [f] $n = 5$. [g] $n = 6$. [h] $n = 7$. [i] $n = 8$. [j] $n = 9$.

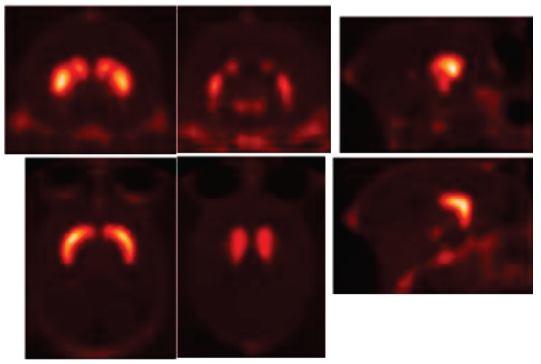

Figure 1. MicroPET images (summed 0−145 min) obtained by injection of [^{18}F]**9** into an anesthetized cynomolgus monkey.

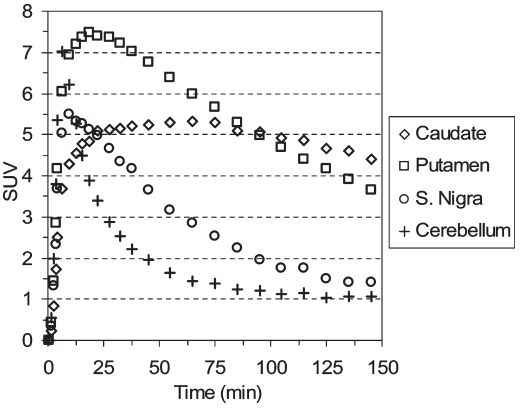

Figure 2. MicroPET baseline TACs obtained by injection of [^{18}F]**9** into an anesthetized cynomolgus monkey.

affinity and display about a 20-fold selectivity over the SERT. This high DAT affinity and moderate SERT affinity is also similar to the *N*-methyl analogues **3** (RTI-31) and **4** (RTI-51), respectively.[87] Compound **13** has a DAT affinity similar to the *N*-methyl analogue **6** (RTI-32)[87] and is about 54 times more selective for the DAT over the SERT. Compound **9** has a reduced DAT affinity relative to compounds **10**−**13**, but the affinity is very similar to the *N*-methyl analogue **2** (the binding affinity determined for **2** is in close agreement with other reported values[22,25,88]), indicating that replacement of the *N*-methyl group with an *N*-(*E*)-fluorobutenyl group does not significantly alter DAT binding. Compound **9** is also more selective for the DAT over the SERT than the other halo-substituted compounds **10**−**12**. All of the *N*-(*E*)-fluorobutenyl tropanes tested have a high DAT vs NET selectivity, with the halo-substituted compounds **9**−**12** displaying a selectivity more than twice that of the methyl-substituted compound **13**.

In Vivo Nonhuman Primate PET Imaging

MicroPET imaging was performed in anesthetized cynomolgus monkeys using a Concorde microPET P4 according to our previously reported procedure.[80] The microPET images for a 145 min baseline study with [^{18}F]**9** are shown in Figure 1, and the time−activity curves (TACs) are shown in Figure 2. As shown by Figures 1 and 2, high uptake of radioactivity is observed in the regions of the brain known to have high DAT density.[7,8] Rapid uptake of [^{18}F]**9** into the putamen is observed (Figure 2), with peak uptake achieved within 20 min followed by a steady washout. Uptake of [^{18}F]**9** in the caudate is less than that observed in the putamen along with a slower rate of uptake and a minimal washout during the first 75 min of the study. Uptake of [^{18}F]**9** in the substantia nigra is rapid, with peak uptake achieved within 10 min followed by a steady washout. Uptake in the cerebellum is rapid, followed by a rapid washout with little or no retention of the tracer as expected for a brain region devoid of DAT. A small amount of radioactivity is also observed in the skull (Figure 1), indicating a low degree of defluorination. This is not surprising because the ^{18}F-radiolabel is in an allylic position, and it has been previously reported that ^{18}F-benzyl fluorides can also undergo defluorination.[89,90] To demonstrate that the uptake of [^{18}F]**9** observed in the baseline study is a result of preferential binding to the DAT, a chase study was performed with the DAT ligand RTI-113·HCl[87,91,92] **19**. As shown in Figure 3, administration of **19** (0.3 mg/kg) at 90 min post-injection results in a complete displacement of [^{18}F]**9**, thus indicating that the observed uptake was a result of binding to the DAT.

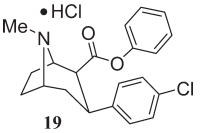

19

MicroPET baseline studies were also performed with [^{18}F]**10**, [^{18}F]**11**, and [^{18}F]**13** (Figures 4−6, respectively). All three tracers show high uptake in the putamen followed by minor washout during the course of the 235 min study. The initial uptake into the putamen is rapid, with peak uptake achieved within 30 min for [^{18}F]**10** and [^{18}F]**11**, and within 55 min for [^{18}F]**13**. Uptake in the caudate is less than that observed in the putamen for [^{18}F]**10**, [^{18}F]**11**, and [^{18}F]**13**, and the rate of uptake is also slower. Furthermore, the uptake in

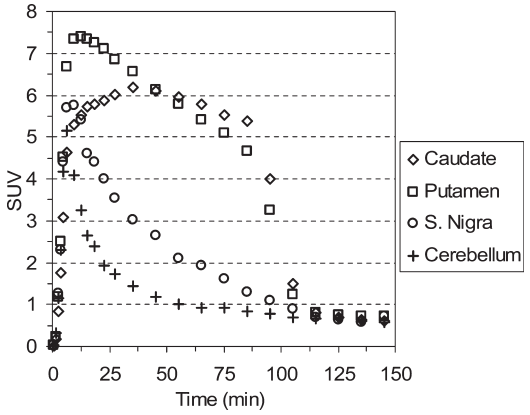

Figure 3. MicroPET TACs showing the result of injection of **19** (0.3 mg/kg) into an anesthetized cynomolgus monkey at 90 min postinjection of [^{18}F]**9**.

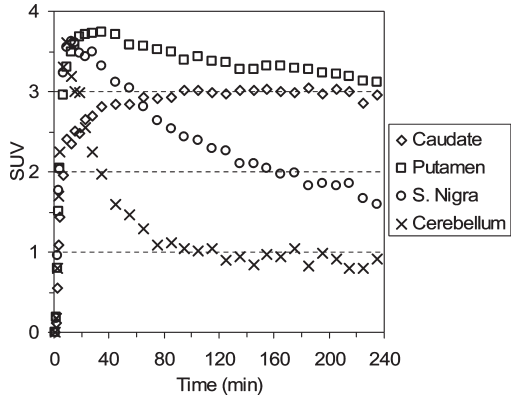

Figure 4. MicroPET baseline TACs obtained by injection of [^{18}F]**10** into an anesthetized cynomolgus monkey.

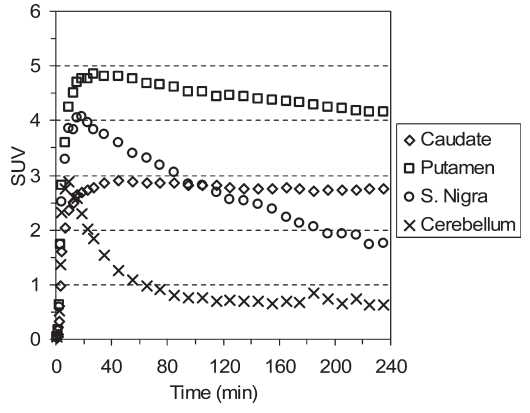

Figure 5. MicroPET baseline TACs obtained by injection of [^{18}F]**11** into an anesthetized cynomolgus monkey.

the caudate fails to wash out during the entire course of the study for [^{18}F]**10**, [^{18}F]**11**, and [^{18}F]**13**. The different levels of uptake of [^{18}F]**13** in the putamen and caudate and the lack of washout are very similar to the results previously reported for [^{11}C]**13** in an anesthetized baboon.[64]

It has been demonstrated in numerous instances that anesthesia can affect the behavior of PET tracers.[93−98] Therefore, an 85 min PET study was performed on a high resolution research tomograph (HRRT) with [^{18}F]**9** in an awake rhesus monkey to determine whether there is a difference between the behavior of [^{18}F]**9** in awake and anesthetized states (Figures 7 and 8).

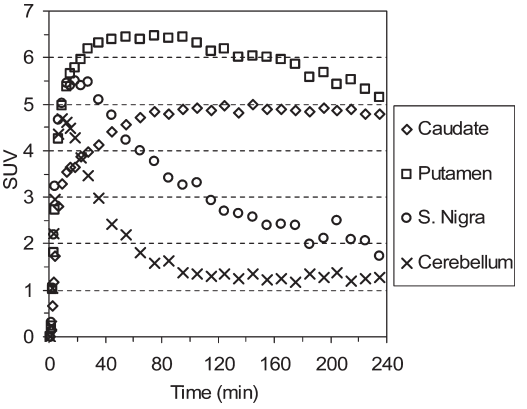

Figure 6. MicroPET baseline TACs obtained by injection of [^{18}F]**13** into an anesthetized cynomolgus monkey.

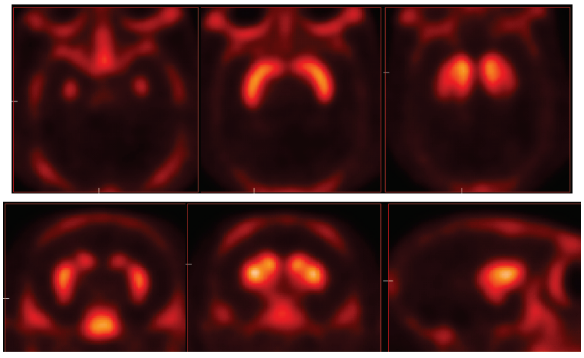

Figure 7. HRRT PET images (summed 55−75 min) obtained by injection of [^{18}F]**9** into an awake rhesus monkey.

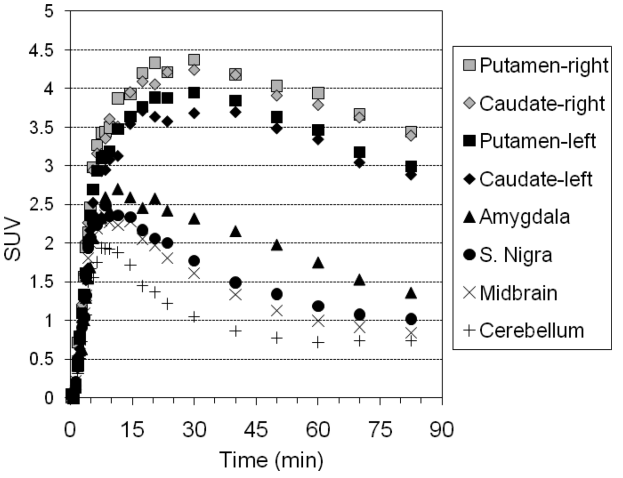

Figure 8. HRRT baseline TACs obtained by injection of [^{18}F]**9** into an awake rhesus monkey.

As shown in Figure 8, the uptake of [^{18}F]**9** is nearly equal in the putamen and caudate in each hemisphere of the awake rhesus monkey brain. This suggests that the different levels of uptake between the putamen and caudate observed in the anesthetized monkey microPET studies shown in Figures 2−6 is due to anesthesia effects. The rate of uptake of [^{18}F]**9** into the putamen and caudate of the awake rhesus monkey is fast, with peak uptake achieved after about 20 min followed by a leveling-off for a period of about 10 min and then a slow but steady washout during which time a quasi-equilibrium[14] is achieved. The kinetic behavior of [^{18}F]**9** in the putamen and

Table 3. Ratio of Uptake of [^{18}F]**9** in the Caudate and Putamen vs Cerebellum Uptake at Selected Time Points for the HRRT Awake Rhesus Monkey Study Shown in Figure 7

time (min)	putamen (left)	caudate (left)	putamen (right)	caudate (right)
30	3.8	3.5	4.2	4.0
40	4.4	4.3	4.8	4.8
50	4.7	4.5	5.2	5.0
60	4.8	4.6	5.5	5.2
70	4.3	4.1	5.0	4.9
82.5	4.0	3.9	4.6	4.6

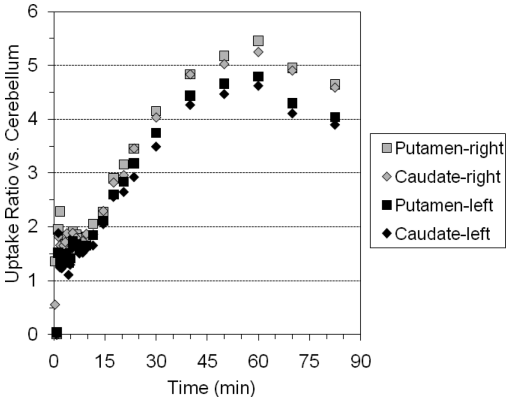

Figure 9. Graph of the ratio of uptake of [^{18}F]**9** in the caudate and putamen vs cerebellum uptake with time for the HRRT awake rhesus monkey study shown in Figure 8.

caudate of the awake monkey is very similar to the kinetic behavior in the putamen of the anesthetized monkey, suggesting that the overall kinetics of [^{18}F]**9** in the putamen are not significantly altered by anesthesia, whereas the different degree of uptake and lack of washout from the caudate in the anesthetized monkey may be the result of anesthesia. On the basis of these results, it is believed that the rate of washout from the putamen for [^{18}F]**10**, [^{18}F]**11**, and [^{18}F]**13** observed in the anesthetized monkey microPET studies would not change significantly in an awake state.

The difference in the rate of washout between [^{18}F]**9**−[^{18}F]**11** and [^{18}F]**13**, aside from any anesthesia effects, is believed to be the result of the different binding affinities shown in Table 2. The DAT is found in high density in the caudate and putamen and, therefore, a very high-affinity ligand is not needed to image the DAT.[99] Compounds **10** and **11** have a subnanomolar affinity for the DAT and compound **13** has an affinity of 2.7 nM, whereas **9** has an affinity of about 9.5 nM. The lower affinity compound [^{18}F]**9** is able to bind to the DAT, then dissociate and wash out, whereas the higher affinity compounds have a delayed washout due to stronger and/or prolonged binding to the DAT in combination with the high density of available binding sites.

Table 3 shows the ratio of uptake in the putamen and caudate vs cerebellum uptake in the awake study with [^{18}F]**9**, and the uptake ratios are plotted vs time in Figure 9. From Table 3 and Figure 9, it can be seen that the highest uptake ratios are obtained after 60 min postinjection and that ratios of ≥4 are maintained for the period 40−80 min postinjection. From the HRRT PET images in Figure 7, it can be seen that the uptake of [^{18}F]**9** is in agreement with the known distribution of DAT in the brain. But, just as was seen with the microPET images in Figure 1, visualization of the skull indicates some degree of defluorination. Compound [^{18}F]**9**, therefore, displays many of the desired properties of an ^{18}F-labeled DAT PET tracer including selectivity for the DAT over the SERT and NET and the achievement of peak uptake and binding equilibrium in a short time frame followed by a steady washout. Unfortunately, a minor degree of defluorination at the allylic position occurs. But, it may be possible to block this defluorination by the administration of disulfiram, which has already been proven to inhibit defluorination of [^{18}F]FCWAY.[100]

Summary

The *N*-(*E*)-fluorobutenyl-3β-(*para*-halo/methyl-phenyl)-nortropanes **9**−**13** were synthesized by reacting the respective nortropane with **14**, which was synthesized in 4 steps from **15**. In vitro competition binding assays demonstrated that **9**−**13** have binding affinities and selectivities similar to their *N*-methyl analogues and that the chloro-, bromo-, and iodo-derivatives **10**−**12**, respectively, bind to the DAT with a 15-fold or greater affinity than the fluoro-derivative **9**. Micro-PET imaging in anesthetized cynomolgus monkeys with [^{18}F]**9**−[^{18}F]**11** and [^{18}F]**13** demonstrated that this very high binding affinity of the chloro-, bromo-, and methyl-derivatives prevented the radiotracer from significantly washing out of the DAT-rich brain regions during the course of the study. This apparent irreversible binding is believed to result from the combination of high DAT affinity of the radiotracer and high DAT density in the putamen and caudate. The lower affinity radiotracer [^{18}F]**9** achieved rapid peak uptake in the putamen followed by a steady washout, whereas uptake in the caudate barely washed out during the course of the study. HRRT PET imaging with [^{18}F]**9** in an awake rhesus monkey showed rapid and high uptake in both the putamen and caudate with peak uptake achieved after 20 min postinjection followed by a steady washout from both the putamen and caudate, thus indicating that the lack of washout in the microPET study was most likely due to an anesthesia effect. Uptake ratios of ≥4 were obtained in the putamen and caudate during the period 40−80 min postinjection of [^{18}F]**9** in the awake study. Thus, in an awake state, [^{18}F]**9** is able to achieve rapid peak uptake in the putamen and caudate with high uptake ratios relative to cerebellum uptake. A minor drawback of the [^{18}F]-fluorobutenyl group is that some degree of defluorination is observed, but it may be possible to prevent this defluorination by administering disulfiram prior to the imaging session.

Experimental Section

General. *trans*-1,4-Dibromo-2-butene (**15**) was purchased from both Acrös and Aldrich. Crystallization of tropanes was performed by stirring a refluxing hexanes solution of the tropane for 10 min, decanting the hot solution into a preheated 25 mL Erlenmeyer flask, capping the flask with a rubber septum, and storing the flask in a freezer (−15 °C). NMR spectra were obtained on Varian Unity and Mercury spectrometers at the specified frequencies. ^{1}H chemical shifts are referenced to internal TMS or residual $CHCl_3$ (7.26 ppm), and ^{13}C chemical shifts are referenced to $CDCl_3$ (77.23 ppm). Silica gel used was EMD Silica Gel 60, 40−63 μm. Vacuum flash chromatography was performed by placing silica in a medium-fritted filter (31 cm length × 4 cm i.d. − Kontes Glassware no. 956250-0044 with adapter no. 205000-2440), eluting under vacuum, and collecting fractions in 125 mL flat-bottomed boiling flasks. Radial chromatography was performed with a Harrison Research Chromatotron. Semipreparative HPLC: Waters XTerra Prep RP_{18}, 5 μm, 19 mm × 100 mm + guard cartridge (19 mm × 10 mm),

60:40:0.1 v/v/v MeOH/H_2O/NEt_3. Analytical HPLC: Waters NovaPak 3.9 mm ×150 mm, 75:25:0.1 v/v/v MeOH/H_2O/NEt_3. HRMS was performed by the Emory University Mass Spectrometry Center. Compound purity was determined by elemental analysis and was found to be >95%. Elemental analysis was performed by Atlantic Microlab, Inc. (www.atlanticmicrolab.com).

***N*-((*E*)-4-Fluorobut-2-en-1-yl)-2β-carbomethoxy-3β-(4′-fluorophenyl)nortropane (9).** Nor-β-CFT[25] (145 mg, 0.55 mmol), **14** (129 mg, 0.53 mmol), *i*-Pr_2NEt (0.12 mL, 0.69 mmol), and $CHCl_3$ (25 mL) were stirred at reflux under $Ar_{(g)}$ for 17 h and then cooled to room temperature. The solution was poured onto dry silica (43 mm h × 43 mm i.d.) and eluted under vacuum: CH_2Cl_2 (25 mL), hexanes (50 mL), hexanes/EtOAc/NEt_3 v/v/v 90:8:2 (50 mL), 75:20:5 (200 mL). The desired fractions were combined, and the solvent was removed to give a yellow syrup that was further purified by radial chromatography (2 mm silica, 98:1:1 v/v/v hexanes/EtOAc/NEt_3 (300 mL)) to afford a colorless syrup (152 mg). Crystallization from refluxing hexanes (3 mL) afforded white crystals (122 mg, 66%). ^{1}H NMR (600 MHz, $CDCl_3$) δ 7.22 (dd, 2 H, *J* = 8.4 Hz, *J* = 5.4 Hz), 6.95 (apparent t, 2 H, *J* = 8.4 Hz), 5.78 (m, 2 H), 4.83 (dd, 2 H, $^2J_{HF}$ = 47.4 Hz, *J* = 4.8 Hz), 3.66 (partially resolved dd, 1 H, *J* = 3.3 Hz, *J* = 6.9 Hz), 3.50 (s, 3 H), 3.43 (m, 1 H), 3.02 (m, 1 H + 1 H overlapping resonances), 2.88 (m, 1 H + 1 H overlapping resonances), 2.60 (td, 1 H, *J* = 12.8 Hz, *J* = 2.6 Hz), 2.10 (m, 1 H), 2.01 (m, 1 H), 1.75 (m, 1 H), 1.66 (m, 2 H). ^{13}C/APT (even +, odd −) NMR (75 MHz, $CDCl_3$) δ 172.07 (+), 161.30 (+, d, $^1J_{CF}$ = 243.6 Hz), 138.75 (+, d, $^4J_{CF}$ = 3.2 Hz), 134.36 (−, d, *J* = 11.8 Hz), 129.00 (−, d, $^3J_{CF}$ = 7.7 Hz), 126.45 (−, d, *J* = 16.6 Hz), 114.85 (−, d, $^2J_{CF}$ = 20.9 Hz), 83.36 (+, d, $^1J_{CF}$ = 161.5 Hz), 62.47 (−), 61.46 (−), 55.09 (+, d, $^4J_{CF}$ = 1.4 Hz), 52.99 (−), 51.21 (−), 34.41 (+), 33.86 (−), 26.24 (+), 26.07 (+). HRMS (APCI) $[MH]^+$ calcd for $C_{19}H_{24}O_2NF_2$, 336.1770, found, 336.1769. Semipreparative HPLC: t_R = 18.9 min (9 mL/min). Analytical HPLC: t_R = 3.9 min (0.95 mL/min). Anal. Calcd for $C_{19}H_{23}F_2NO_2$: C, 68.04; H, 6.91; N, 4.18. Found: C, 68.09; H, 6.91; N, 4.26.

***N*-((*E*)-4-[^{18}F]Fluorobut-2-en-1-yl)-2β-carbomethoxy-3β-(4′-fluorophenyl)nortropane ([^{18}F]9).** Nor-β-CFT[25] (~1.9 mg) was dissolved in DMF (0.3 mL) and added to the V-tube containing [^{18}F]**14**. The mixture was heated at 105 °C for 15 min and then cooled in a 0 °C ice bath for 1 min. The mixture was diluted with HPLC solvent (~0.5 mL) and purified by semipreparative HPLC (9.1 mL/min; t_R = 17−21 min (range)). The desired fractions were combined, diluted 1:1.5 v/v with H_2O, and collected on a Waters C_{18} Sep-Pak. The Sep-Pak was rinsed with 0.9% saline (35 mL) and then EtOH (0.5 mL). The product was eluted from the Sep-Pak with EtOH (1.5 mL) and collected in a sealed sterile vial containing 0.9% $NaCl_{(aq)}$ (3.5 mL). This solution was passed successively through a 1 μm filter and then a 0.2 μm filter (Acrodisc PTFE) under Ar-pressure and collected in a sealed sterile dose vial containing 0.9% $NaCl_{(aq)}$ (10 mL). The total synthesis time was ~1 h from addition of the nortropane to [^{18}F]**14** with a 24% radiochemical yield (decay corrected). The product was then analyzed by analytical HPLC (t_R = 3.8 min, 1 mL/min) to determine the radiochemical purity (99%) and specific activity (SA = 851 mCi/μmol).

Compounds **10**−**13** were prepared in a similar manner as compound **9**. Compounds [^{18}F]**10** (SA = 3859 mCi/μmol), [^{18}F]**11** (SA = 1440 mCi/μmol), and [^{18}F]**13** (SA: not determined) were prepared in a similar manner as [^{18}F]**9**.

***N*-((*E*)-4-Fluorobut-2-en-1-yl)-2β-carbomethoxy-3β-(4′-chlorophenyl)nortropane (10).** White needle crystals (22 mg, 21%). ^{1}H NMR (600 MHz, $CDCl_3$) δ 7.23 (d, 2 H, *J* = 9.0 Hz), 7.19 (d, 2 H, *J* = 9.0 Hz), 5.78 (m, 2 H), 4.83 (dd, 2 H, $^2J_{HF}$ = 47.4 Hz, *J* = 5.4 Hz), 3.67 (partially resolved dd, 1 H, *J* = 6.9 Hz, *J* = 2.7 Hz), 3.50 (s, 3 H), 3.42 (m, 1 H), 3.01 (m, 1 H + 1 H, overlapping resonances), 2.88 (m, 1 H + 1 H, overlapping resonances), 2.58 (td, 1 H, *J* = 12.6 Hz, *J* = 3.0 Hz), 2.10 (m, 1 H), 2.01 (m, 1 H), 1.74 (m, 1 H), 1.66 (m, 2 H). ^{13}C NMR (75 MHz, $CDCl_3$) δ 172.01, 141.74, 134.33 (d, *J* = 11.5 Hz), 131.71, 128.95, 128.23, 126.48 (d, *J* = 16.6 Hz), 83.36 (d, *J* = 161.7 Hz), 62.49, 61.39, 55.09 (d, *J* = 1.4 Hz), 52.86, 51.26, 34.20, 33.97, 26.24, 26.06. HRMS (APCI) $[MH]^+$ calcd for $C_{19}H_{24}O_2N^{35}ClF$, 352.1474; found, 352.1473. Anal. Calcd for $C_{19}H_{23}ClFNO_2$: C, 64.86; H 6.59; N, 3.98. Found: C, 64.81; H, 6.63; N, 3.97. Semipreparative HPLC: t_R = 28.5 min (9 mL/min).

***N*-((*E*)-4-Fluorobut-2-en-1-yl)-2β-carbomethoxy-3β-(4′-bromophenyl)nortropane (11).** White needle crystals (20 mg, 19%). ^{1}H NMR (300 MHz, $CDCl_3$) δ 7.38 (d, 2 H, *J* = 8.4 Hz), 7.14 (d, 2 H, *J* = 8.4 Hz), 5.78 (m, 2 H), 4.83 (partially resolved dd, 2 H, $^2J_{HF}$ = 47.3 Hz, *J* = 4.8 Hz), 3.67 (m, 1 H), 3.50 (s, 3 H), 3.42 (m, 1 H), 2.96 (m, 4 H, overlapping resonances), 2.58 (td, 1 H, *J* = 12.5 Hz, *J* = 2.8 Hz), 2.06 (m, 2 H), 1.69 (m, 3 H). ^{13}C NMR (75 MHz, $CDCl_3$) δ 171.99, 142.29, 134.33 (d, *J* = 11.8 Hz), 131.17, 129.38, 126.48 (d, *J* = 17.2 Hz), 119.85, 83.36 (d, *J* = 161.7 Hz), 62.49, 61.38, 55.10 (d, *J* = 1.4 Hz), 51.28, 34.14, 34.05, 26.24, 26.06. HRMS (APCI) $[MH]^+$ calcd for $C_{19}H_{24}O_2N^{79}BrF$, 396.0969; found, 396.0969. Anal. Calcd for $C_{19}H_{23}BrFNO_2$: C, 57.58; H, 5.85; N, 3.53. Found: C, 58.41; H, 5.88; N, 3.62. Semipreparative HPLC: t_R = 33.0 min (9 mL/min).

***N*-((*E*)-4-Fluorobut-2-en-1-yl)-2β-carbomethoxy-3β-(4′-iodophenyl)nortropane (12).** White solid (117 mg, 69%). ^{1}H NMR (300 MHz, $CDCl_3$) δ 7.58 (d, 2 H, *J* = 8.4 Hz), 7.02 (d, 2 H, *J* = 8.4 Hz), 5.78 (m, 2 H), 4.83 (partially resolved dd, 2 H, $^2J_{HF}$ = 47.1 Hz, *J* = 4.8 Hz), 3.67 (m, 1 H), 3.50 (s, 3 H), 3.42 (m, 1 H), 2.95 (m, 4 H, overlapping resonances), 2.57 (td, 1 H, *J* = 12.4 Hz, *J* = 2.8 Hz), 2.05 (m, 2 H), 1.69 (m, 3 H). ^{13}C NMR (75 MHz, $CDCl_3$) δ 171.97, 143.01, 137.11, 134.31 (d, *J* = 11.8 Hz), 129.72, 126.47 (d, *J* = 16.6 Hz), 91.34, 83.34 (d, *J* = 161.7 Hz), 62.46, 61.35, 55.07 (d, *J* = 1.4 Hz), 52.74, 51.27, 34.10, 34.01, 26.24, 26.03. HRMS (APCI) $[MH]^+$ calcd for $C_{19}H_{24}O_2NF^{127}I$, 444.0830; found, 444.0830. Anal. Calcd for $C_{19}H_{23}FINO_2$: C, 51.48; H, 5.23; N, 3.16. Found: C, 52.07; H, 5.24; N, 3.23. Semipreparative HPLC: t_R = 46.6 min (9 mL/min).

***N*-((*E*)-4-Fluorobut-2-en-1-yl)-2β-carbomethoxy-3β-(4′-methylphenyl)nortropane (13).** Colorless syrup (would not crystallize from hexanes) (23 mg, 53%). ^{1}H NMR (300 MHz, $CDCl_3$) δ 7.16 (d, 2 H, *J* = 8.1 Hz), 7.08 (d, 2 H, *J* = 8.1 Hz), 5.79 (m, 2 H), 4.83 (partially resolved dd, 2 H, $^2J_{HF}$ = 47.3 Hz, *J* = 4.8 Hz), 3.66 (m, 1 H), 3.49 (s, 3 H), 3.42 (m, 1 H), 3.01 (m, 1 H + 1 H, overlapping resonances), 2.88 (m, 1 H + 1 H, overlapping resonances), 2.61 (td, 1 H, *J* = 12.6 Hz, *J* = 3.0 Hz), 2.29 (s, 3 H), 2.04 (m, 2 H), 1.70 (m, 3 H). HRMS (APCI) $[MH]^+$ calcd for $C_{20}H_{27}O_2NF$, 332.2020; found, 332.2020. Anal. Calcd for $C_{20}H_{26}FNO_2$: C, 72.48; H, 7.91; N, 4.23. Found: C, 72.40; H, 7.86; N, 4.25.

(*E*)-4-Fluoro-1-tosyloxy-2-butene (14). (*E*)-1,4-Ditosyloxy-2-butene (**18**) (256 mg, 0.65 mmol), Bu_4NF (1 M in THF, 0.7 mL), and THF (10 mL) were stirred at reflux under $Ar_{(g)}$ for 30 min. The solvent was removed and the residue was purified by flash column chromatography on silica (2:1 v/v hexanes/EtOEt) to afford a colorless oil (60 mg, 38%). ^{1}H NMR (300 MHz, $CDCl_3$) δ 7.80 (d, 2 H, *J* = 8.4 Hz), 7.36 (d, 2 H, *J* = 8.4 Hz), 5.99−5.75 (m, 2 H), 4.84 (ddd, 2 H, $^2J_{FH}$ = 46.5 Hz, *J* = 4.8 Hz, *J* = 1.2 Hz), 4.57 (m, 2 H), 2.46 (s, 3 H).

(*E*)-4-[^{18}F]Fluoro-1-tosyloxy-2-butene ([^{18}F]14). $H^{18}F$ was produced with a Siemens 11-MeV RDS 112 cyclotron by employing the $^{18}O(p,n)^{18}F$ reaction in $H_2{}^{18}O$. The $H^{18}F_{(aq)}$ was transferred to a chemical processing control unit (CPCU), collected on a trap/release cartridge, released with $K_2CO_{3(aq)}$ (0.9 mg in 0.6 mL H_2O), and combined with a CH_3CN solution of Kryptofix-222 (5 mg in 1 mL) in a V-tube. The V-tube was placed in a 110 °C oil bath, the solvent was evaporated under a $N_{2(g)}$ flow, and CH_3CN (3 mL) was added and evaporated in order to azeotropically dry the Kryptofix-222/$K^{18}F$ complex. (*E*)-1,4-Ditosyloxy-2-butene (**18**) (4 mg in 1 mL CH_3CN) was added, the reaction mixture was heated at 90 °C for 10 min, and [^{18}F]**14** was trapped on a Waters silica Sep-Pak Classic (WAT051900) (previously prepped with 10 mL of EtOEt). Compound [^{18}F]**14** was eluted with EtOEt, and the EtOEt

solution was transferred to a hot cell under $N_{2(g)}$ pressure and collected in a V-tube. The V-tube was placed in an 80 °C oil bath and the EtOEt was evaporated with an $Ar_{(g)}$ flow. The solution of radiolabeling precursor was then added to this V-tube.

(*E*)-1,4-Diacetoxy-2-butene (16). *trans*-1,4-Dibromo-2-butene (**15**) (1.98 g, 9.26 mmol), KOAc (4.70 g, 47.89 mmol, 5.2 equiv), and AcOH (25 mL) were stirred at reflux under $Ar_{(g)}$ for 21 h. The mixture was cooled to room temperature, filtered, the precipitate was rinsed with toluene, and the AcOH was removed from the filtrate azeotropically with toluene to give a wet white solid that was dried under vacuum for ~10 min. The solid was suspended in CH_2Cl_2 and purified by vacuum flash chromatography on silica (13 cm h × 4 cm i.d.): hexanes (100 mL), v/v hexanes/CH_2Cl_2 − 3:1 (200 mL), 1:1 (200 mL), 1:3 (200 mL), CH_2Cl_2 (900 mL), to afford a colorless oil (1.04 g, 65%). TLC R_f = 0.4 (silica, CH_2Cl_2, I_2 vapor). ^{1}H NMR (300 MHz, $CDCl_3$) δ 5.86 (septet, 2 H, J = 1.4 Hz), 4.58 (dd, 4 H, J = 1.4 Hz), 2.08 (s, 6 H). ^{13}C NMR (75 MHz, $CDCl_3$) δ 170.86, 128.23, 64.07, 21.08.

(*E*)-1,4-Dihydroxy-2-butene (17). (*E*)-1,4-Diacetoxy-2-butene (**16**) (2.08 g, 12.08 mmol), HCl (2.0 M EtOEt, 0.9 mL, 1.8 mmol, 0.15 equiv), and EtOH (75 mL) were stirred at reflux under $Ar_{(g)}$ for 16 h, cooled, and the solvent was removed to afford a faint yellow oil (1.04 g, 98%). ^{1}H NMR (300 MHz, $CDCl_3$) δ 5.90 (m, 2 H), 4.18 (m, 4 H).

(*E*)-1,4-Ditosyloxy-2-butene (18). (*E*)-1,4-Dihydroxy-2-butene (**17**) (326 mg, 3.70 mmol), *p*-toluenesulfonyl chloride (1.76 g, 9.23 mmol, 2.5 equiv), and THF (30 mL) were combined and cooled to 0 °C under $Ar_{(g)}$ followed by addition of sodium *t*-butoxide (1.07 g, 11.13 mmol, 3.0 equiv) in portions. The reaction mixture was stirred at room temperature overnight followed by addition of H_2O (100 mL) and then extraction with CH_2Cl_2 (25 mL × 3). The combined CH_2Cl_2 extracts were dried over $MgSO_4$ and the solvent was removed. The crude product was purified by flash column chromatography on silica (3:1:1 v/v/v hexanes/EtOEt/CH_2Cl_2) to afford white crystals (1.21 g, 82%). ^{1}H NMR (300 MHz, $CDCl_3$) δ 7.77 (d, 4 H, J = 8.4 Hz), 7.35 (d, 4 H, J = 8.4 Hz), 5.74 (m, 2 H), 4.48 (m, 4 H), 2.46 (s, 6 H).

Acknowledgment. This research was sponsored by the NIMH (1-R21-MH-66622-01). We acknowledge the use of shared instrumentation provided by grants from the NIH and the NSF. Lauryn M. Daniel thanks the Behavioral Research Advancements in Neuroscience (BRAIN) program, part of the Center for Behavioral Neuroscience (www.cbn-atl.org), for a summer research opportunity.

References

(1) Thie, J. A. Understanding the Standardized Uptake Value, Its Methods, and Implications for Usage. *J. Nucl. Med.* **2004**, *45*, 1431–1434.
(2) Bentourkia, M.; Zaidi, H. Tracer Kinetic Modeling in PET. *PET Clin.* **2007**, *2*, 267–277.
(3) Giros, B.; El Mestikawy, S.; Godinot, N.; Zheng, K.; Han, H.; Yang-Feng, T.; Caron, M. G. Cloning, Pharmacological Characterization, and Chromosome Assignment of the Human Dopamine Transporter. *Mol. Pharmacol.* **1992**, *42*, 383–390.
(4) Nelson, N. The Family of Na^+/Cl^- Neurotransmitter Transporters. *J. Neurochem.* **1998**, *71*, 1785–1803.
(5) Eisenhofer, G. The Role of Neuronal and Extraneuronal Plasma Membrane Transporters in the Inactivation of Peripheral Catecholamines. *Pharmacol. Ther.* **2001**, *91*, 35–62.
(6) Torres, G. E.; Gainetdinov, R. R.; Caron, M. G. Plasma Membrane Monoamine Transporters: Structure, Regulation and Function. *Nat. Rev. Neurosci.* **2003**, *4*, 13–25.
(7) Nirenberg, M. J.; Vaughan, R. A.; Uhl, G. R.; Kuhar, M. J.; Pickel, V. M. The Dopamine Transporter is Localized to Dendritic and Axonal Plasma Membranes of Nigrostriatal Dopaminergic Neurons. *J. Neurosci.* **1996**, *16*, 436–447.
(8) Ciliax, B. J.; Drash, G. W.; Staley, J. K.; Haber, S.; Mobley, C. J.; Miller, G. W.; Mufson, E. J.; Mash, D. C.; Levey, A. I. Immunocytochemical Localization of the Dopamine Transporter in Human Brain. *J. Comp. Neurol.* **1999**, *409*, 38–56.
(9) Niznik, H. B.; Fogel, E. F.; Fassos, F. F.; Seeman, P. The Dopamine Transporter Is Absent in Parkinsonian Putamen and Reduced in the Caudate Nucleus. *J. Neurochem.* **1991**, *56*, 192–198.
(10) Chinaglia, G.; Alvarez, F. J.; Probst, A.; Palacios, J. M. Mesostriatal and Mesolimbic Dopamine Uptake Binding Sites are Reduced in Parkinson's Disease and Progressive Supranuclear Palsy: A Quantitative Autoradiographic Study Using [^{3}H]Mazindol. *Neuroscience* **1992**, *49*, 317–327.
(11) Dawson, T. M.; Dawson, V. L. Molecular Pathways of Neurodegeneration in Parkinson's Disease. *Science* **2003**, *302*, 819–822.
(12) Mazei-Robison, M. S.; Couch, R. S.; Shelton, R. C.; Stein, M. A.; Blakely, R. D. Sequence Variation in the Human Dopamine Transporter Gene in Children with Attention Deficit Hyperactivity Disorder. *Neuropharmacology* **2005**, *49*, 724–736.
(13) Singer, H. S.; Hahn, I.-H.; Moran, T. H. Abnormal Dopamine Uptake Sites in Postmortem Striatum from Patients with Tourette's Syndrome. *Ann. Neurol.* **1991**, *30*, 558–562.
(14) Laruelle, M.; Slifstein, M.; Huang, Y. Positron Emission Tomography: Imaging and Quantification of Neurotransporter Availability. *Methods* **2002**, *27*, 287–299.
(15) Talbot, P. S.; Laruelle, M. The Role of In Vivo Molecular Imaging with PET and SPECT in the Elucidation of Psychiatric Drug Action and New Drug Development. *Eur. Neuropsychopharmacol.* **2002**, *12*, 503–511.
(16) Lee, C.-M.; Farde, L. Using Positron Emission Tomography to Facilitate CNS Drug Development. *Trends Pharmacol. Sci.* **2006**, *27*, 310–316.
(17) Ritz, M. C.; Lamb, R. J.; Goldberg, S. R.; Kuhar, M. J. Cocaine Receptors on Dopamine Transporters Are Related to Self-Administration of Cocaine. *Science* **1987**, *237*, 1219–1223.
(18) Scheffel, U.; Boja, J. W.; Kuhar, M. J. Cocaine Receptors: In Vivo Labeling with ^{3}H-(−)-Cocaine, ^{3}H-WIN 35,065-2, and ^{3}H-WIN 35,428. *Synapse* **1989**, *4*, 390–392.
(19) Carroll, F. I.; Howell, L. L.; Kuhar, M. J. Pharmacotherapies for Treatment of Cocaine Abuse: Preclinical Aspects. *J. Med. Chem.* **1999**, *42*, 2721–2736.
(20) Carroll, F. I. 2002 Medicinal Chemistry Division Award Address: Monoamine Transporters and Opioid Receptors. Targets for Addiction Therapy. *J. Med. Chem.* **2003**, *46*, 1775–1794.
(21) Clarke, R. L.; Daum, S. J.; Gambino, A. J.; Aceto, M. D.; Pearl, J.; Levitt, M.; Cumiskey, W. R.; Bogado, E. F. Compounds Affecting the Central Nervous System. 4. 3β-Phenyltropane-2-carboxylic Esters and Analogs. *J. Med. Chem.* **1973**, *16*, 1260–1267.
(22) Boja, J. W.; Carroll, F. I.; Rahman, M. A.; Philip, A.; Lewin, A. H.; Kuhar, M. J. New, Potent Cocaine Analogs: Ligand Binding and Transport Studies in Rat Striatum. *Eur. J. Pharmacol.* **1990**, *184*, 329–332.
(23) Boja, J. W.; Patel, A.; Carroll, F. I.; Rahman, M. A.; Philip, A.; Lewin, A. H.; Kopajtic, T. A.; Kuhar, M. J. [^{125}I]RTI-55: A Potent Ligand for Dopamine Transporters. *Eur. J. Pharmacol.* **1991**, *194*, 133–134.
(24) Carroll, F. I.; Gao, Y.; Rahman, M. A.; Abraham, P.; Parham, K.; Lewin, A. H.; Boja, J. W.; Kuhar, M. J. Synthesis, Ligand Binding, QSAR, and CoMFA Study of 3β-(*p*-Substituted phenyl)tropane-2β-carboxylic Acid Methyl Esters. *J. Med. Chem.* **1991**, *34*, 2719–2725.
(25) Meltzer, P. C.; Liang, A. Y.; Brownell, A.-L.; Elmaleh, D. R.; Madras, B. K. Substituted 3-Phenyltropane Analogs of Cocaine: Synthesis, Inhibition of Binding at Cocaine Recognition Sites, and Positron Emission Tomography Imaging. *J. Med. Chem.* **1993**, *36*, 855–862.
(26) Wilson, A. A.; DaSilva, J. N.; Houle, S. In Vivo Evaluation of [^{11}C]- and [^{18}F]-Labelled Cocaine Analogues as Potential Dopamine Transporter Ligands for Positron Emission Tomography. *Nucl. Med. Biol.* **1996**, *23*, 141–146.
(27) Lundkvist, C.; Halldin, C.; Swahn, C.-G.; Ginovart, N.; Farde, L. Different Brain Radioactivity Curves in a PET Study with [^{11}C]β-CIT Labelled in Two Different Positions. *Nucl. Med. Biol.* **1999**, *26*, 343–350.
(28) Yoder, K. K.; Hutchins, G. D.; Mock, B. H.; Fei, X.; Winkle, W. L.; Gitter, B. D.; Territo, P. R.; Zheng, Q.-H. Dopamine Transporter Binding in Rat Striatum: A Comparison of [*O*-methyl-^{11}C]β-CFT and [*N*-methyl-^{11}C]β-CFT. *Nucl. Med. Biol.* **2009**, *36*, 11–16.
(29) Ametamey, S. M.; Honer, M.; Schubiger, P. A. Molecular Imaging with PET. *Chem. Rev.* **2008**, *108*, 1501–1516.
(30) Wernick, M. N.; Aarsvold, J. N. *Emission Tomography: The Fundamentals of PET and SPECT*; Elsevier Academic Press: San Diego, CA; London, UK, 2004.
(31) Levin, C. S.; Hoffman, E. J. Calculation of Positron Range and Its Effect on the Fundamental Limit of Positron Emission

Tomography System Spatial Resolution. *Phys. Med. Biol.* **1999**, *44*, 781–799.
(32) Böhm, H.-J.; Banner, D.; Bendels, S.; Kansy, M.; Kuhn, B.; Müller, K.; Obst-Sander, U.; Stahl, M. Fluorine in Medicinal Chemistry. *ChemBioChem* **2004**, *5*, 637–643.
(33) Sun, S.; Adejare, A. Fluorinated Molecules as Drugs and Imaging Agents in the CNS. *Curr. Top. Med. Chem.* **2006**, *6*, 1457–1464.
(34) Müller, K.; Faeh, C.; Diederich, F. Fluorine in Pharmaceuticals: Looking Beyond Intuition. *Science* **2007**, *317*, 1881–1886.
(35) Hagmann, W. K. The Many Roles for Fluorine in Medicinal Chemistry. *J. Med. Chem.* **2008**, *51*, 4359–4369.
(36) Cai, L.; Lu, S.; Pike, V. W. Chemistry with [^{18}F]Fluoride Ion. *Eur. J. Org. Chem.* **2008**, 2853–2873.
(37) Prakash, G. K. S.; Hu, J. Selective Fluoroalkylations with Fluorinated Sulfones, Sulfoxides, and Sulfides. *Acc. Chem. Res.* **2007**, *40*, 921–930.
(38) Kirk, K. L. Fluorination in Medicinal Chemistry: Methods, Strategies, and Recent Developments. *Org. Process Res. Dev.* **2008**, *12*, 305–321.
(39) Haaparanta, M.; Bergman, J.; Laakso, A.; Hietala, J.; Solin, O. [^{18}F]CFT ([^{18}F]WIN 35,428), A Radioligand to Study the Dopamine Transporter With PET: Biodistribution in Rats. *Synapse* **1996**, *23*, 321–327.
(40) Laakso, A.; Bergman, J.; Haaparanta, M.; Vilkman, H.; Solin, O.; Hietala, J. [^{18}F]CFT ([^{18}F]WIN 35,428), A Radioligand to Study the Dopamine Transporter With PET: Characterization in Human Subjects. *Synapse* **1998**, *28*, 244–250.
(41) Stehouwer, J. S.; Goodman, M. M. Fluorine-18 Radiolabeled PET Tracers for Imaging Monoamine Transporters: Dopamine, Serotonin, and Norepinephrine. *PET Clin.* **2009**, *4*, 101–128.
(42) Goodman, M. M.; Kilts, C. D.; Keil, R.; Shi, B.; Martarello, L.; Xing, D.; Votaw, J.; Ely, T. D.; Lambert, P.; Owens, M. J.; Camp, V. M.; Malveaux, E.; Hoffman, J. M. ^{18}F-Labeled FECNT: A Selective Radioligand for PET Imaging of Brain Dopamine Transporters. *Nucl. Med. Biol.* **2000**, *27*, 1–12.
(43) Lundkvist, C.; Halldin, C.; Ginovart, N.; Swahn, C.-G.; Farde, L. [^{18}F]β-CIT-FP Is Superior to [^{11}C]β-CIT-FP for Quantitation of the Dopamine Transporter. *Nucl. Med. Biol.* **1997**, *24*, 621–627.
(44) Deterding, T. A.; Votaw, J. R.; Wang, C. K.; Eshima, D.; Eshima, L.; Keil, R.; Malveaux, E.; Kilts, C. D.; Goodman, M. M.; Hoffman, J. M. Biodistribution and Radiation Dosimetry of the Dopamine Transporter Ligand [^{18}F]FECNT. *J. Nucl. Med.* **2001**, *42*, 376–381.
(45) Tipre, D. N.; Fujita, M.; Chin, F. T.; Seneca, N.; Vines, D.; Liow, J.-S.; Pike, V. W.; Innis, R. B. Whole-Body Biodistribution and Radiation Dosimetry Estimates for the PET Dopamine Transporter Probe ^{18}F-FECNT in Nonhuman Primates. *Nucl. Med. Commun.* **2004**, *25*, 737–742.
(46) Davis, M. R.; Votaw, J. R.; Bremner, J. D.; Byas-Smith, M. G.; Faber, T. L.; Voll, R. J.; Hoffman, J. M.; Grafton, S. T.; Kilts, C. D.; Goodman, M. M. Initial Human PET Imaging Studies with the Dopamine Transporter Ligand ^{18}F-FECNT. *J. Nucl. Med.* **2003**, *44*, 855–861.
(47) Chaly, T.; Dhawan, V.; Kazumata, K.; Antonini, A.; Margouleff, C.; Dahl, J. R.; Belakhlef, A.; Margouleff, D.; Yee, A.; Wang, S.; Tamagnan, G.; Neumeyer, J. L.; Eidelberg, D. Radiosynthesis of [^{18}F]*N*-3-Fluoropropyl-2-β-carbomethoxy-3-β-(4-iodophenyl) Nortropane and the First Human Study With Positron Emission Tomography. *Nucl. Med. Biol.* **1996**, *23*, 999–1004.
(48) Kazumata, K.; Dhawan, V.; Chaly, T.; Antonini, A.; Margouleff, C.; Belakhlef, A.; Neumeyer, J.; Eidelberg, D. Dopamine Transporter Imaging with Fluorine-18-FPCIT and PET. *J. Nucl. Med.* **1998**, *39*, 1521–1530.
(49) Robeson, W.; Dhawan, V.; Belakhlef, A.; Ma, Y.; Pillai, V.; Chaly, T.; Margouleff, C.; Bjelke, D.; Eidelberg, D. Dosimetry of the Dopamine Transporter Radioligand ^{18}F-FPCIT in Human Subjects. *J. Nucl. Med.* **2003**, *44*, 961–966.
(50) Yaqub, M.; Boellaard, R.; van Berckel, B. N. M.; Ponsen, M. M.; Lubberink, M.; Windhorst, A. D.; Berendse, H. W.; Lammertsma, A. A. Quantification of Dopamine Transporter Binding Using [^{18}F]FP-β-CIT and Positron Emission Tomography. *J. Cereb. Blood Flow Metab.* **2007**, *27*, 1397–1406.
(51) Laruelle, M. The Role of Model-Based Methods in the Development of Single Scan Techniques. *Nucl. Med. Biol.* **2000**, *27*, 637–642.
(52) Logan, J. Graphical Analysis of PET Data Applied to Reversible and Irreversible Tracers. *Nucl. Med. Biol.* **2000**, *27*, 661–670.
(53) Neumeyer, J. L.; Tamagnan, G.; Wang, S.; Gao, Y.; Milius, R. A.; Kula, N. S.; Baldessarini, R. J. *N*-Substituted Analogs of 2β-Carbomethoxy-3β-(4′-iodophenyl)tropane (β-CIT) with Selective Affinity to Dopamine or Serotonin Transporters in Rat Forebrain. *J. Med. Chem.* **1996**, *39*, 543–548.
(54) Goodman, M. M.; Keil, R.; Shoup, T. M.; Eshima, D.; Eshima, L.; Kilts, C.; Votaw, J.; Camp, V. M.; Votaw, D.; Smith, E.; Kung, M.-P.; Malveaux, E.; Watts, R.; Huerkamp, M.; Wu, D.; Garcia, E.; Hoffman, J. M. Fluorine-18-FPCT: A PET Radiotracer for Imaging Dopamine Transporters. *J. Nucl. Med.* **1997**, *38*, 119–126.
(55) Koivula, T.; Marjamäki, P.; Haaparanta, M.; Fagerholm, V.; Grönroos, T.; Lipponen, T.; Perhola, O.; Vepsäläinen, J.; Solin, O. Ex Vivo Evaluation of *N*-(3-[^{18}F]Fluoropropyl)-2β-carbomethoxy-3β-(4-fluorophenyl)nortropane in Rats. *Nucl. Med. Biol.* **2008**, *35*, 177–183.
(56) Wang, J. L.; Parhi, A. K.; Oya, S.; Lieberman, B.; Kung, M.-P.; Kung, H. F. 2-(2′-((Dimethylamino)methyl)-4′-(3-[^{18}F]fluoropropoxy)-phenylthio)benzenamine for Positron Emission Tomography Imaging of Serotonin Transporters. *Nucl. Med. Biol.* **2008**, *35*, 447–458.
(57) Zoghbi, S. S.; Shetty, U.; Ichise, M.; Fujita, M.; Imaizumi, M.; Liow, J.-S.; Shah, J.; Musachio, J. L.; Pike, V. W.; Innis, R. B. PET Imaging of the Dopamine Transporter with ^{18}F-FECNT: A Polar Radiometabolite Confounds Brain Radioligand Measurements. *J. Nucl. Med.* **2006**, *47*, 520–527.
(58) Luurtsema, G.; Schuit, R. C.; Takkenkamp, K.; Lubberink, M.; Hendrikse, N. H.; Windhorst, A. D.; Molthoff, C. F. M.; Tolboom, N.; van Berckel, B. N. M.; Lammertsma, A. A. Peripheral Metabolism of [^{18}F]FDDNP and Cerebral Uptake of its Labelled Metabolites. *Nucl. Med. Biol.* **2008**, *35*, 869–874.
(59) Chen, P.; Kilts, C. D.; Camp, V. M.; Ely, T. D.; Keil, R.; Malveaux, E.; Votaw, J.; Hoffman, J. M.; Goodman, M. M. Synthesis, characterization and in vivo evaluation of (*N*-(*E*)-4-[^{18}F]fluorobut-2-en-1-yl)-2β-carbomethoxy-3β-(4-substitutedphenyl)nortropanes for imaging DAT by PET. *J. Labelled Compd. Radiopharm.* **1999**, *42* (Suppl 1), S400.
(60) Goodman, M. M.; Chen, P. Fluoroalkenyl Nortropanes. U.S. Patent US 6,344,179 B1, Feb 5, 2002.
(61) Goodman, M. M.; Kung, M.-P.; Kabalka, G. W.; Kung, H. F.; Switzer, R. Synthesis and Characterization of Radioiodinated *N*-(3-Iodopropen-1-yl)-2β-carbomethoxy-3β-(4-chlorophenyl)-tropanes: Potential Dopamine Reuptake Site Imaging Agents. *J. Med. Chem.* **1994**, *37*, 1535–1542.
(62) Malison, R. T.; Vessotskie, J. M.; Kung, M.-P.; McElgin, W.; Romaniello, G.; Kim, H.-J.; Goodman, M. M.; Kung, H. F. Striatal Dopamine Transporter Imaging in Nonhuman Primates with Iodine-123-IPT SPECT. *J. Nucl. Med.* **1995**, *36*, 2290–2297.
(63) Kim, H.-J.; Im, J.-H.; Yang, S.-O.; Moon, D. H.; Ryu, J. S.; Bong, J.-K.; Nam, K.-P.; Cheon, J.-H.; Lee, M.-C.; Lee, H. K. Imaging and Quantitation of Dopamine Transporters with Iodine-123-IPT in Normal and Parkinson's Disease Subjects. *J. Nucl. Med.* **1997**, *38*, 1703–1711.
(64) Chalon, S.; Hall, H.; Saba, W.; Garreau, L.; Dollé, F.; Halldin, C.; Emond, P.; Bottlaender, M.; Deloye, J.-B.; Helfenbein, J.; Madelmont, J.-C.; Bodard, S.; Mincheva, Z.; Besnard, J.-C.; Guilloteau, D. Pharmacological Characterization of (*E*)-*N*-(4-Fluorobut-2-enyl)-2β-carbomethoxy-3β-(4′-tolyl)nortropane (LBT-999) as a Highly Promising Fluorinated Ligand for the Dopamine Transporter. *J. Pharmacol. Exp. Ther.* **2006**, *317*, 147–152.
(65) Riss, P. J.; Hummerich, R.; Schloss, P. Synthesis and Monoamine Uptake Inhibition of Conformationally Constrained 2β-Carbomethoxy-3β-phenyl Tropanes. *Org. Biomol. Chem.* **2009**, *7*, 2688–2698.
(66) Riss, P. J.; Debus, F.; Hummerich, R.; Schmidt, U.; Schloss, P.; Lueddens, H.; Roesch, F. Ex Vivo and In Vivo Evaluation of [^{18}F]PR04.MZ in Rodents: A Selective Dopamine Transporter Imaging Agent. *ChemMedChem* **2009**, *4*, 1480–1487.
(67) Stehouwer, J. S.; Chen, P.; Voll, R. J.; Williams, L.; Votaw, J. R.; Howell, L. L.; Goodman, M. M. PET Imaging of the Dopamine Transporter with [^{18}F]FBFNT. *J. Labelled Compd. Radiopharm.* **2007**, *50* (Suppl. 1), S335.
(68) Boja, J. W.; Kuhar, M. J.; Kopajtic, T.; Yang, E.; Abraham, P.; Lewin, A. H.; Carroll, F. I. Secondary Amine Analogues of 3β-(4′-Substituted phenyl)tropane-2β-carboxylic Acid Esters and *N*-Norcocaine Exhibit Enhanced Affinity for Serotonin and Norepinephrine Transporters. *J. Med. Chem.* **1994**, *37*, 1220–1223.
(69) Raphael, R. A. Synthesis of Carbohydrates by Use of Acetylenic Precursors. Part II. Addition Reactions of *cis*- and *trans*-But-2-ene-1,4-diol Diacetates. Synthesis of DL-Erythrulose. *J. Chem. Soc.* **1952**, 401–405.
(70) Bouquillon, S.; Muzart, J. Palladium(0)-Catalyzed Isomerization of (*Z*)-1,4-Diacetoxy-2-butene—Dependence of η^1- η^3-Allylpalladium as a Key Intermediate on the Solvent Polarity. *Eur. J. Org. Chem.* **2001**, 3301–3305.

(71) Organ, M. G.; Cooper, J. T.; Rogers, L. R.; Soleymanzadeh, F.; Paul, T. Synthesis of Stereodefined Polysubstituted Olefins. 1. Sequential Intermolecular Reactions Involving Selective, Stepwise Insertion of Pd(0) into Allylic and Vinylic Halide Bonds. The Stereoselective Synthesis of Disubstituted Olefins. *J. Org. Chem.* **2000**, *65*, 7959–7970.
(72) Miller, A. E. G.; Biss, J. W.; Schwartzman, L. H. Reductions with Dialkylaluminum Hydrides. *J. Org. Chem.* **1959**, *24*, 627–630.
(73) Dollé, F.; Emond, P.; Mavel, S.; Demphel, S.; Hinnen, F.; Mincheva, Z.; Saba, W.; Valette, H.; Chalon, S.; Halldin, C.; Helfenbein, J.; Legaillard, J.; Madelmont, J.-C.; Deloye, J.-B.; Bottlaender, M.; Guilloteau, D. Synthesis, radiosynthesis and in vivo preliminary evaluation of [^{11}C]LBT-999, a selective radioligand for the visualisation of the dopamine transporter with PET. *Bioorg. Med. Chem.* **2006**, *14*, 1115–1125.
(74) Baldwin, S. W.; Jeffs, P. W.; Natarajan, S. Preparation of Norcocaine. *Synth. Commun.* **1977**, *7*, 79–84.
(75) Lemaire, C.; Plenevaux, A.; Aerts, J.; Del Fiore, G.; Brihaye, C.; Le Bars, D.; Comar, D.; Luxen, A. Solid Phase Extraction—An Alternative to the Use of Rotary Evaporators for Solvent Removal in the Rapid Formulation of PET Radiopharmaceuticals. *J. Labelled Compd. Radiopharm.* **1999**, *42*, 63–75.
(76) Dischino, D. D.; Welch, M. J.; Kilbourn, M. R.; Raichle, M. E. Relationship Between Lipophilicity and Brain Extraction of C-11-Labeled Radiopharmaceuticals. *J. Nucl. Med.* **1983**, *24*, 1030–1038.
(77) Waterhouse, R. N. Determination of Lipophilicity and Its Use as a Predictor of Blood−Brain Barrier Penetration of Molecular Imaging Agents. *Mol. Imaging Biol.* **2003**, *5*, 376–389.
(78) Wilson, A. A.; Houle, S. Radiosynthesis of Carbon-11 Labelled *N*-Methyl-2-(arylthio)benzylamines: Potential Radiotracers for the Serotonin Reuptake Receptor. *J. Labelled Compd. Radiopharm.* **1999**, *42*, 1277–1288.
(79) Wilson, A. A.; Jin, L.; Garcia, A.; DaSilva, J. N.; Houle, S. An Admonition When Measuring the Lipophilicity of Radiotracers Using Counting Techniques. *Appl. Radiat. Isot.* **2001**, *54*, 203–208.
(80) Plisson, C.; McConathy, J.; Martarello, L.; Malveaux, E. J.; Camp, V. M.; Williams, L.; Votaw, J. R.; Goodman, M. M. Synthesis, Radiosynthesis, and Biological Evaluation of Carbon-11 and Iodine-123 Labeled 2β-Carbomethoxy-3β-[4′-((*Z*)-2-haloethenyl)phenyl]tropanes: Candidate Radioligands for in Vivo Imaging of the Serotonin Transporter. *J. Med. Chem.* **2004**, *47*, 1122–1135.
(81) Owens, M. J.; Morgan, W. N.; Plott, S. J.; Nemeroff, C. B. Neurotransmitter Receptor and Transporter Binding Profile of Antidepressants and Their Metabolites. *J. Pharmacol. Exp. Ther.* **1997**, *283*, 1305–1322.
(82) Hyttel, J.; Bøgesø, K. P.; Perregaard, J.; Sánchez, C. The Pharmacological Effect of Citalopram Resides in the (*S*)-(+)-Enantiomer. *J. Neural Transm.* **1992**, *88*, 157–160.
(83) Lee, C. M.; Javitch, J. A.; Snyder, S. H. Characterization of [^{3}H]Desipramine Binding Associated with Neuronal Norepinephrine Uptake Sites in Rat Brain Membranes. *J. Neurosci.* **1982**, *2*, 1515–1525.
(84) Duncan, G. E.; Little, K. Y.; Kirkman, J. A.; Kaldas, R. S.; Stumpf, W. E.; Breese, G. R. Autoradiographic Characterization of [^{3}H]Imipramine and [^{3}H]Citalopram Binding in Rat and Human Brain: Species Differences and Relationships to Serotonin Innervation Patterns. *Brain Res.* **1992**, *591*, 181–197.
(85) Cheetham, S. C.; Viggers, J. A.; Butler, S. A.; Prow, M. R.; Heal, D. J. [^{3}H]Nisoxetine—A Radioligand for Noradrenaline Reuptake Sites: Correlation with Inhibition of [^{3}H]Noradrenaline Uptake and Effects of DSP-4 Lesioning and Antidepressant Treatments. *Neuropharmacology* **1996**, *35*, 63–70.
(86) Neumeyer, J. L.; Wang, S.; Milius, R. A.; Baldwin, R. M.; Zea-Ponce, Y.; Hoffer, P. B.; Sybirska, E.; Al-Tikriti, M.; Charney, D. S.; Malison, R. T.; Laruelle, M.; Innis, R. B. [^{123}I]-2β-Carbomethoxy-3β-(4-iodophenyl)tropane: High-Affinity SPECT Radiotracer of Monoamine Reuptake Sites in Brain. *J. Med. Chem.* **1991**, *34*, 3144–3146.
(87) Carroll, F. I.; Kotian, P.; Dehghani, A.; Gray, J. L.; Kuzemko, M. A.; Parham, K. A.; Abraham, P.; Lewin, A. H.; Boja, J. W.; Kuhar, M. J. Cocaine and 3β-(4′-Substituted phenyl)tropane-2β-carboxylic Acid Ester and Amide Analogues. New High-Affinity and Selective Compounds for the Dopamine Transporter. *J. Med. Chem.* **1995**, *38*, 379–388.
(88) Kuhar, M. J.; McGirr, K. M.; Hunter, R. G.; Lambert, P. D.; Garrett, B. E.; Carroll, F. I. Studies of Selected Phenyltropanes at Monoamine Transporters. *Drug Alcohol Depend.* **1999**, *56*, 9–15.
(89) Petric, A.; Barrio, J. R.; Namavari, M.; Huang, S.-C.; Satyamurthy, N. Synthesis of 3β-(4-[^{18}F]Fluoromethylphenyl)- and 3β-2-[^{18}F]Fluoromethylphenyl)tropane-2β-Carboxylic Acid Methyl Esters: New Ligands for Mapping Brain Dopamine Transporter With Positron Emission Tomography. *Nucl. Med. Biol.* **1999**, *26*, 529–535.
(90) Stout, D.; Petric, A.; Satyamurthy, N.; Nguyen, Q.; Huang, S.-C.; Namavari, M.; Barrio, J. R. 2β-Carbomethoxy-3β-(4- and 2-[^{18}F]Fluoromethylphenyl)tropanes: Specific Probes for in Vivo Quantification of Central Dopamine Transporter Sites. *Nucl. Med. Biol.* **1999**, *26*, 897–903.
(91) Cook, C. D.; Carroll, F. I.; Beardsley, P. M. RTI 113, a 3-Phenyltropane Analog, Produces Long-Lasting Cocaine-Like Discriminative Stimulus Effects in Rats and Squirrel Monkeys. *Eur. J. Pharmacol.* **2002**, *442*, 93–98.
(92) Kimmel, H. L.; Negus, S. S.; Wilcox, K. M.; Ewing, S. B.; Stehouwer, J.; Goodman, M. M.; Votaw, J. R.; Mello, N. K.; Carroll, F. I.; Howell, L. L. Relationship Between Rate of Drug Uptake in Brain and Behavioral Pharmacology of Monoamine Transporter Inhibitors in Rhesus Monkeys. *Pharmacol., Biochem. Behav.* **2008**, *90*, 453–462.
(93) Tsukada, H.; Nishiyama, S.; Kakiuchi, T.; Ohba, H.; Sato, K.; Harada, N.; Nakanishi, S. Isoflurane Anesthesia Enhances the Inhibitory Effects of Cocaine and GBR12909 on Dopamine Transporter: PET Studies in Combination with Microdialysis in the Monkey Brain. *Brain Res.* **1999**, *849*, 85–96.
(94) Mizugaki, M.; Nakagawa, N.; Nakamura, H.; Hishinuma, T.; Tomioka, Y.; Ishiwata, S.; Ido, T.; Iwata, R.; Funaki, Y.; Itoh, M.; Higuchi, M.; Okamura, N.; Fujiwara, T.; Sato, M.; Shindo, K.; Yoshida, S. Influence of Anesthesia on Brain Distribution of [^{11}C]Methamphetamine in Monkeys in Positron Emission Tomography (PET) Study. *Brain Res.* **2001**, *911*, 173–175.
(95) Tsukada, H.; Nishiyama, S.; Kakiuchi, T.; Ohba, H.; Sato, K.; Harada, N. Ketamine Alters the Availability of Striatal Dopamine Transporter as Measured by [^{11}C]β-CFT and [^{11}C]β-CIT-FE in the Monkey Brain. *Synapse* **2001**, *42*, 273–280.
(96) Elfving, B.; Bjørnholm, B.; Knudsen, G. M. Interference of Anaesthetics With Radioligand Binding in Neuroreceptor Studies. *Eur. J. Nucl. Med. Mol. Imaging* **2003**, *30*, 912–915.
(97) Votaw, J.; Byas-Smith, M.; Hua, J.; Voll, R.; Martarello, L.; Levey, A. I.; Bowman, F. D.; Goodman, M. Interaction of Isoflurane With the Dopamine Transporter. *Anesthesiology* **2003**, *98*, 404–411.
(98) Votaw, J. R.; Byas-Smith, M. G.; Voll, R.; Halkar, R.; Goodman, M. M. Isoflurane Alters the Amount of Dopamine Transporter Expressed on the Plasma Membrane in Humans. *Anesthesiology* **2004**, *101*, 1128–1135.
(99) Eckelman, W. C.; Kilbourn, M. R.; Mathis, C. A. Discussion of Targeting Proteins In Vivo: In Vitro Guidelines. *Nucl. Med. Biol.* **2006**, *33*, 449–451.
(100) Ryu, Y. H.; Liow, J.-S.; Zoghbi, S.; Fujita, M.; Collins, J.; Tipre, D.; Sangare, J.; Hong, J.; Pike, V. W.; Innis, R. B. Disulfiram Inhibits Defluorination of ^{18}F-FCWAY, Reduces Bone Radioactivity, and Enhances Visualization of Radioligand Binding to Serotonin 5-HT$_{1A}$ Receptors in Human Brain. *J. Nucl. Med.* **2007**, *48*, 1154–1161.